

## An efficient heterogeneous Fenton catalyst based on modified diatomite for degradation of cationic dye simulated wastewater

Shengyan Pu<sup>a,b,\*</sup>, Chunyan Xiang<sup>a</sup>, Rongxin Zhu<sup>a</sup>, Hui Ma<sup>a,\*</sup>, Anatoly Zinchenko<sup>a,c</sup>, Wei Chu<sup>b,\*</sup>

<sup>a</sup>State Key Laboratory of Geohazard Prevention and Geoenvironment Protection (Chengdu University of Technology), 1#, Dongsanlu, Erxianqiao, Chengdu 610059, Sichuan, China, email: pushengyan@gmail.com

<sup>b</sup>Department of Civil and Environment Engineering, The Hong Kong Polytechnic University, Hong Kong, China

<sup>c</sup>Graduate School of Environmental Studies, Nagoya University, Nagoya 464-8601, Japan

Received 18 December 2016; Accepted 13 April 2017

### ABSTRACT

Heterogeneous catalysts overcome the drawbacks of the homogeneous Fenton process, and have attracted considerable attention for degradation of organic pollutants in wastewater. In this study, a heterogeneous Fenton catalyst system was developed for the degradation of cationic dye by incorporating ferric oxide nanoparticles into modified diatomite composite. The catalyst was synthesized through two simple steps: firstly, the raw diatomite was modified by soaking into nitric acid; then, through forced hydrolysis strategy, the ferric oxide nanoparticles were incorporated into the pre-treated diatomite. The resultant catalyst were characterized by X-ray diffraction, scanning electron microscopy, and energy dispersive X-ray spectroscopy. This novel diatomite-Fe<sub>2</sub>O<sub>3</sub> catalyst demonstrated distinct catalytic activity and desirable efficiency for degradation of organic dye. Methylene Blue (MB) was completely decomposed within 20 min, and the decomposition efficiency was remained higher than 90% after 5 cycles of catalyst regeneration. The simplicity and low cost of the demonstrated catalytic material is promising for the efficient degradation of organic pollutants.

**Keywords:** Modified diatomite; Fenton degradation; Heterogeneous catalyst; Methylene blue; Cationic dye wastewater

### 1. Introduction

Dye wastewater has become one of the major industrial water pollution sources in developing countries [1]. For instance, over  $1.6 \times 10^9$  m<sup>3</sup> dye wastewater is generated in China every year. Dye wastewater contains high concentrations of unfixed dyes, salts, and other organic compounds [2]. Particularly, cationic dyes are amongst most common pollutants in the dye-containing wastewaters [3]. The dyes are usually resistant to conventional degradation methods such as biological wastewater treatment [4–6]. Different kinds of treatment processes have been applied to the treatment. Advanced oxida-

tion processes (AOPs) are efficient methods to degrade refractory organic pollutants, as they can generate ·OH radical ( $E = 2.8$  V), a powerful oxidant which has been widely recognized to effectively oxidize most organic pollutants into harmless compounds, such as CO<sub>2</sub>, H<sub>2</sub>O, and organic acids, such as formic acid, acetic and oxalic acid [7]. Among the AOPs, the classical Fenton reaction, which utilizes an aqueous mixture of ionic iron (Fe<sup>2+</sup>/Fe<sup>3+</sup>) and hydrogen peroxide (H<sub>2</sub>O<sub>2</sub>), emerges to be a promising remediation technology due to its low toxicity, fast reaction rates and simplicity of control [8]. However, the conventional homogeneous Fenton process has a number of critical drawbacks. First, the high concentration (50–80 ppm) of leached iron ions in the treated effluent can result in the formation of coagulated slud-

\*Corresponding authors.

ges [9]. Second, the homogeneous Fenton reaction has to be carried out under strict control of pH value in a narrow range between 2 and 4 [10]. Therefore, these inevitable disadvantages limit its board applications in water treatment [11].

To overcome these defect, heterogeneous Fenton systems and related reaction encompassing the reactions of  $H_2O_2$  with solid iron-based catalysts have been proposed as promising alternatives to the homogeneous Fenton processes. The heterogeneous Fenton catalysts can avoid sludge formation from iron ions, extend the effective pH range, and enhance the generation of highly potent oxidizing hydroxyl radicals [12]. To date, various supports such as aluminosilicate minerals [13–15] and activated carbon [16] have been developed as Fenton-catalyst. Diatomite, known as diatomaceous earth or bio-silica, consists of about 90% silicone dioxide along with small quantities of alumina and iron oxide. Compared to other matrixes, diatomite is a more promising candidate to be used in the synthesis of heterogeneous catalyst [17]. As a highly microporous silicon material, diatomite benefits from high capacity of adsorption, a uniform pore size distribution, a large surface area [18], desirable hydrophilicity and decent chemical stability [19,20]. In addition, diatomite of various structures is easier to handle compared to granular supports [21]. However, the thermal treatment significantly decreases diatomite surface area and the pores of raw diatomite are always blocked by carbonate [18]. In recent years the heterogeneous Fenton -like reaction- has been thoughtfully studied to modify the surface characteristic of diatomite by acid or base treatments [22]. Acid treatment may increase surface area and the concentration of these medium acid sites [23].

Based on these remarkable properties of diatomite, this study focused on a novel D- $Fe_2O_3$  heterogeneous Fenton catalyst which was fabricated through a simple forced hydrolysis method to enhance the catalytic performance. The catalytic properties of D- $Fe_2O_3$  were evaluated by the degradation of cationic-dye wastewater in the presence of  $H_2O_2$ . In this paper, Methylene Blue (MB) was selected as a model contaminant and a representative modern cationic-dye with low biodegradability in water treatment systems. Several reaction systems were systematically investigated, along with the factors that may influence the removal of dyes such as dosage, initial pH, reaction temperature, and catalyst stability.

## 2. Materials and methods

### 2.1. Materials

The raw diatomite powder, ferric nitrate ( $Fe(NO_3)_3 \cdot 9H_2O$ ,  $\geq 98.5\%$ ), nitric acid ( $HNO_3$ , 65–68%), sodium hydroxide ( $NaOH$ ,  $\geq 98\%$ ), sulfuric acid ( $H_2SO_4$ , 98%) were obtained from Chengdu Kelong Chemical Reagent Company (Sichuan, China). Hydrogen peroxide ( $H_2O_2$ , 30 wt%) was supplied by Tianjin Zhiyuan Chemical Reagent Company (Tianjin, China). All reagents were used as received with no further purification. All solutions were prepared with distilled deionized water (18.25 M/cm), obtained with a Milli-Q Water Purification System (Ulupure Corporation, Chengdu).

### 2.2. Preparation of diatomite- $Fe_2O_3$

The heterogeneous catalyst applied in catalytic ozonation was prepared by a impregnation method. Prior to  $Fe_2O_3$  coating, the raw diatomite was modified with  $HNO_3$  solution for purification. The mixture was mechanically stirred at room temperature for 4 h, filtered, washed with deionized water for several times, and finally dried at  $110^\circ C$ . The above process was repeated three times to steadily modify catalyst loading.

Diatomite- $Fe_2O_3$  compound was synthesized based on a simple forced hydrolysis method as shown in Fig.1.

In brief, different amounts of modified diatomite powder was added into a vigorously stirred 0.5 M solution of  $Fe(NO_3)_3$ . The solid-to-liquid ratio was set at 1:10 (wt%). After 60 min of stirring, the suspension was heated to  $95^\circ C$  until the suspension evaporated to slurry. Subsequently, the slurry was dried at  $110^\circ C$  for 5 h. The as-prepared catalyst was obtained after washing, filtering and stoving. During the preparation, the catalyst was repeatedly washed until the iron ions were not detected by flame atomic absorption spectrometry.

### 2.3. Characterization

Scanning electron microscopy (SEM) images were obtained using an S-3000N field emission scanning electron microscope (Hitachi, Japan) equipped with an energy dispersive X-ray (EDX) spectroscopy. The composition and crystallinity of the samples were characterized by powder X-ray diffraction patterns (XRD) on a DX-2700 X-Ray diffractometer using  $Cu-K\alpha$  radiation ( $\lambda = 1.540562 \text{ \AA}$ , 40 kV, 30 mA) as the X-ray source at a scanning rate of  $3^\circ/\text{min}$  in the range of  $3^\circ$  to  $80^\circ$ .

### 2.4. Catalytic test

The catalytic activities of the modified diatomite and diatomite- $Fe_2O_3$  were studied in order to evaluate their effectiveness in degradation of MB in aqueous solution. For the degradation of MB, a certain amount of diatomite- $Fe_2O_3$  catalyst was suspended in a 250 mL of MB (50 mg/L) aqueous solution and the pH value was adjusted by  $H_2SO_4/NaOH$  solution. The pH was not controlled by buffer solutions during the oxidation experiments. Before the reaction, the suspension was sufficiently sonicated for 10 min to disperse the catalyst and the reaction temperature was maintained at different temperature by water bath. Next, a certain amount of  $H_2O_2$  (30%) aqueous solution was gently added to the reaction solution. About 3 mL of the sample was collected at each given reaction time, filtered through a  $0.25 \mu m$  filter and analyzed immediately using a V-1100D UV-vis spectrophotometer (Shanghai United Instrument Co., Ltd, China) at a wavelength of 665 nm.

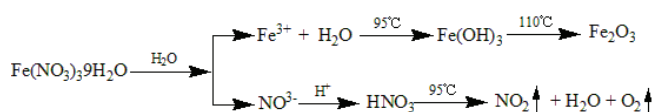


Fig. 1. Reaction flow chart of Diatomite- $Fe_2O_3$  catalyst preparation.

The decoloration efficiency (DE%) was calculated to evaluate the degradation effect based on the following formula:

$$DE\% = (C_0 - C_t) / C_0 \times 100\% \quad (1)$$

where  $C_0$  (mg/L) is the initial concentration of MB and  $C$  (mg/L) is the remaining concentration of MB after reaction. All the batch experiments were conducted in duplicates and the results showed that the experimental errors were less than 5%.

### 3. Results and discussion

#### 3.1. Preparation of heterogeneous Fenton catalyst

The modified diatomite and ferric nitrate mixture was first heated to 95°C to form  $\text{Fe}(\text{OH})_3$  and then the composite was dried at 110°C to form  $\text{Fe}_2\text{O}_3$  loaded on the diatomite. The preparation process of the D- $\text{Fe}_2\text{O}_3$  is shown in Fig. 2A. The modified diatomite appeared as a milky white powder. The D- $\text{Fe}_2\text{O}_3$  was still of powder morphology, except that the color became dark brown indicating the presence of iron oxide. A schematic illustration of the D- $\text{Fe}_2\text{O}_3$  preparation as well as the degradation of cationic dye by heterogeneous catalysis of  $\text{H}_2\text{O}_2/\text{D-Fe}_2\text{O}_3$  system is shown in Fig. 2B. The diatomite-Fe mixture was heated to 95°C to trigger the hydrolysis reaction to form  $\text{Fe}(\text{OH})_3$ , then dried at 110°C to

form  $\text{Fe}_2\text{O}_3$ . During the reaction, the extra  $\text{H}^+$  was evaporated in the form of  $\text{HNO}_3$ .

Next, the micromorphology of the prepared catalyst was studied by scanning electron microscopy (SEM). SEM images of the modified diatomite and D- $\text{Fe}_2\text{O}_3$  are shown in Fig. 3. The structure of the modified diatomite is characterized by the extraordinary diversity of size, shapes, morphology and organization of diatomite particles. The material had a highly porous, discoid morphology as depicted in Fig. 3A and 3C, showing an array of ordered circular pores of discoid structure with a diameter around 350 nm. Fig. 3B and 3D were images of the prepared catalyst showing similar structure to the modified diatomite except that the surface was densely deposited with dispersed  $\text{Fe}_2\text{O}_3$  compared to Fig. 3C. Most importantly, it indicated that  $\text{Fe}_2\text{O}_3$  was not simply mixed with but fully coated onto the diatomite, which was in favor of the catalytic activity.

Next, the purity and phase of the modified diatomite and D- $\text{Fe}_2\text{O}_3$  were characterized by XRD, as shown in Fig. 4A. Curve (a) indicates that the peaks in the XRD pattern of the modified diatomite was in a good agreement with the pure phase of  $\text{SiO}_2$ . The peaks at  $2\theta = 22.052, 36.165$  corresponded to  $\text{SiO}_2$  and were characteristic of diatomite comparing to the standard card (75-0923). Curve (b) corresponded to XRD pattern of  $\text{Fe}_2\text{O}_3$  nanoparticles formed on the surface of the modified diatomite. The emerging signals at 21.073, 26.667, 35.147, 45.251 and 48.499, indicated the existence of goethite ( $\text{FeO}(\text{OH})$ ) and ferric oxide ( $\text{Fe}_2\text{O}_3$ ). Shape similarity of curve (a) and curve (b) indicated that the

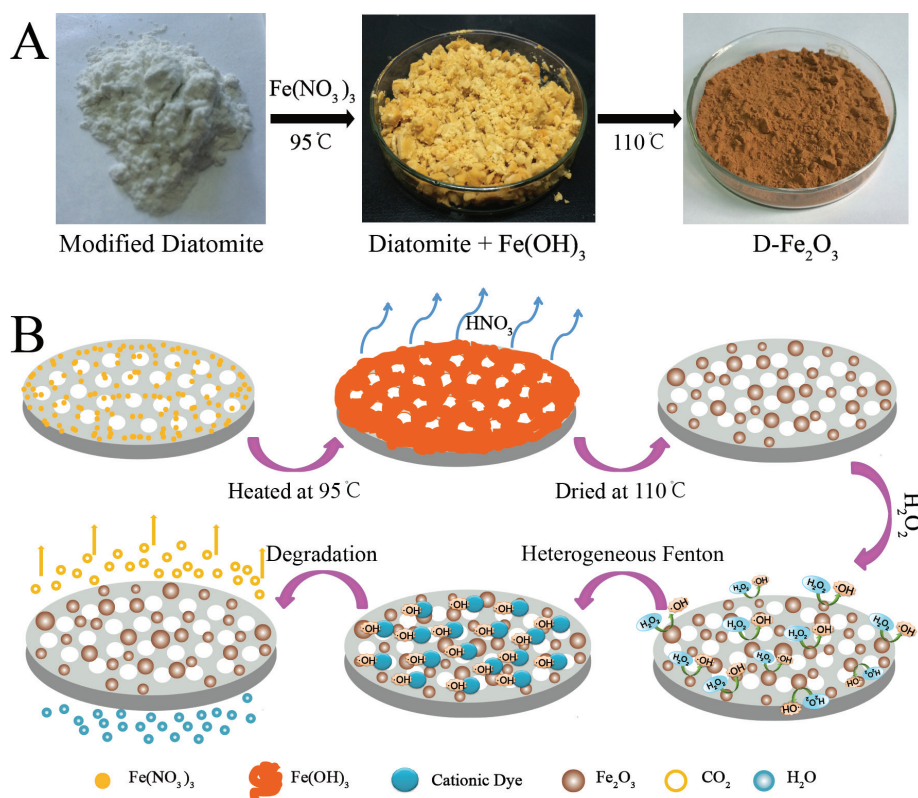


Fig. 2. A) Photographs of diatomite-based materials at different steps of D- $\text{Fe}_2\text{O}_3$  preparation; B) Schematic illustration of the D- $\text{Fe}_2\text{O}_3$  preparation and degradation of cationic dye by heterogeneous catalysis in  $\text{H}_2\text{O}_2/\text{D-Fe}_2\text{O}_3$  system.

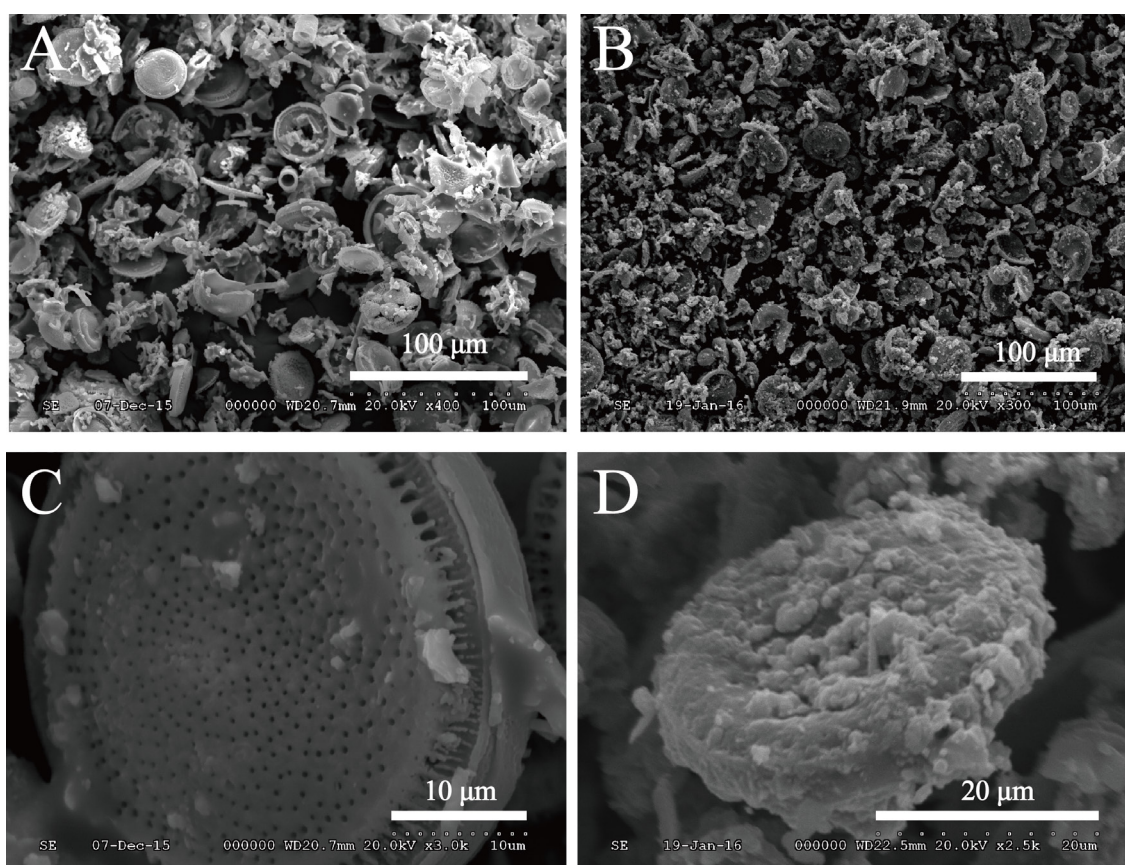


Fig. 3. SEM images of the modified diatomite (A and C) and diatomite-Fe<sub>2</sub>O<sub>3</sub> catalyst (B and D).

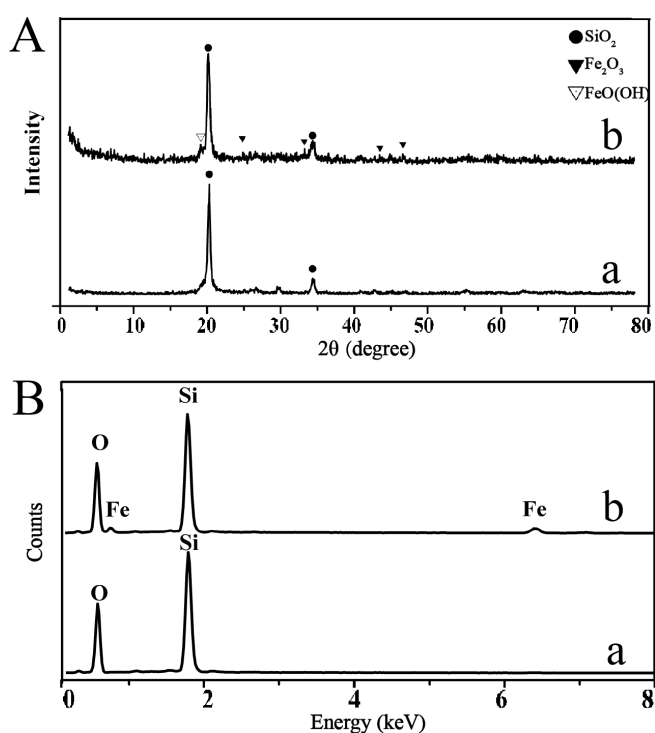


Fig. 4. A) XRD patterns of diatomite (a), D-Fe<sub>2</sub>O<sub>3</sub> (b); B) EDX patterns of diatomite (a), D-Fe<sub>2</sub>O<sub>3</sub> (b).

structure of D-Fe<sub>2</sub>O<sub>3</sub> was similar to the modified diatomite. This Figure indicated that Fe<sub>2</sub>O<sub>3</sub> has been successfully coated on the surface of diatomite. Most importantly, this evolution of Fe<sub>2</sub>O<sub>3</sub> coated diatomite was speculated to be acting favorably for a high catalytic activity during the degradation of organic dye solution, as described further below. XRD patterns indicated the crystal form of the Fe<sub>2</sub>O<sub>3</sub> was not very stable, which gave the possibility to release iron ions into Fenton reaction systems.

In order to further confirm the existence of Fe<sub>2</sub>O<sub>3</sub> in D-Fe<sub>2</sub>O<sub>3</sub> composite, the corresponding EDX analysis of the modified diatomite and D-Fe<sub>2</sub>O<sub>3</sub> were carried out and the results are shown in Fig. 4B. EDX pattern of modified diatomite indicated the presence of silicon oxide, which was in agreement with the XRD results. Spectrum (b) showed two other peaks that corresponded to the presence of iron oxide. As expected, the pattern confirmed the presences of Si, Fe and O within D-Fe<sub>2</sub>O<sub>3</sub> composite. No other elements were detected in the EDX spectrum.

### 3.2. Degradation of MB by diatomite-Fe<sub>2</sub>O<sub>3</sub> catalyst

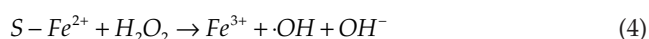
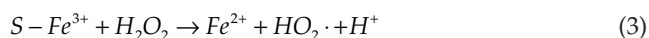
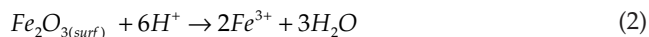
The performance of D-Fe<sub>2</sub>O<sub>3</sub> as heterogeneous Fenton catalyst was tested by the degradation of MB aqueous solution (50 mg/L) under several operating conditions. The experiments were performed using various reaction systems (D-Fe<sub>2</sub>O<sub>3</sub>/H<sub>2</sub>O<sub>2</sub>, diatomite, D-Fe<sub>2</sub>O<sub>3</sub>, H<sub>2</sub>O<sub>2</sub> and Fe<sup>2+</sup>/H<sub>2</sub>O<sub>2</sub>), catalyst dosages (2, 4, 6, 8, 10 and 12 g/L),

reaction temperature (25, 35, 45, and 55°C), H<sub>2</sub>O<sub>2</sub> concentrations (20, 40, 60, 80, 100, and 120 mmol/L), and initial pH (3, 4, 5, 6, and 7).

### 3.2.1. Performance of the reaction system

Different systems of H<sub>2</sub>O<sub>2</sub>, D-Fe<sub>2</sub>O<sub>3</sub>, modified diatomite, conventional Fe<sup>2+</sup>/H<sub>2</sub>O<sub>2</sub> and heterogeneous D-Fe<sub>2</sub>O<sub>3</sub>/H<sub>2</sub>O<sub>2</sub> were evaluated at 55°C, with the H<sub>2</sub>O<sub>2</sub> concentration of 120 mmol/L, and initial pH of 3. The dosage of D-Fe<sub>2</sub>O<sub>3</sub>, modified diatomite and heterogeneous D-Fe<sub>2</sub>O<sub>3</sub>/H<sub>2</sub>O<sub>2</sub> were 12 g/L, respectively. As illustrated in Fig. 5A, adding H<sub>2</sub>O<sub>2</sub> or D-Fe<sub>2</sub>O<sub>3</sub> compound alone to the MB solution had nearly no degradation effect during the 90 min reaction time. Due to the porous structure and high specific surface area, the modified diatomite could remove a certain amount of pollutant through adsorption, and the decoloration efficiency was about 30% after equilibrium reached. In heterogeneous Fenton system composed of D-Fe<sub>2</sub>O<sub>3</sub> and H<sub>2</sub>O<sub>2</sub>, the dye (MB) could be efficiently removed and fully degraded (>99.9%) within 20 min. The result revealed that H<sub>2</sub>O<sub>2</sub> alone could hardly oxidize and break the MB molecules, and the adsorption capacity of D-Fe<sub>2</sub>O<sub>3</sub> compound was much lower than the modified diatomite since the Fe<sub>2</sub>O<sub>3</sub> loading on surface blocks its surface pores to a great extent. However, the degradation efficiency greatly increased in heterogeneous Fenton system (H<sub>2</sub>O<sub>2</sub>/D-Fe<sub>2</sub>O<sub>3</sub>), since H<sub>2</sub>O<sub>2</sub> could be efficiently decomposed under catalysis of the loading ferric

oxide and produce hydroxyl radicals ( $\cdot\text{OH}$ ) to attack the pollutant molecules according to Eq. (2)–(4) [24].



S: Catalyst surface

The iron ions in heterogeneous system fully produced through the reaction between D-Fe<sub>2</sub>O<sub>3</sub> and H<sub>2</sub>O<sub>2</sub>. The reaction rate increased by 4.5 times in the heterogeneous system compared to the conventional homogeneous Fenton system (Fe<sup>2+</sup>/H<sub>2</sub>O<sub>2</sub>) under the same iron ion concentration (3 mg/L).

### 3.2.2. Effect of the H<sub>2</sub>O<sub>2</sub> concentration

The H<sub>2</sub>O<sub>2</sub> concentration effect was evaluated at 55°C, with D-Fe<sub>2</sub>O<sub>3</sub> dosage of 12 g/L, initial pH of 3 and with a H<sub>2</sub>O<sub>2</sub> concentration of 0, 20, 40, 60, 80, 100, and 120 mmol/L, respectively. As shown in Fig. 5B, the highest removal efficiency of H<sub>2</sub>O<sub>2</sub> free system was 4% which is mainly attributed to the adsorption effect. Under constant iron

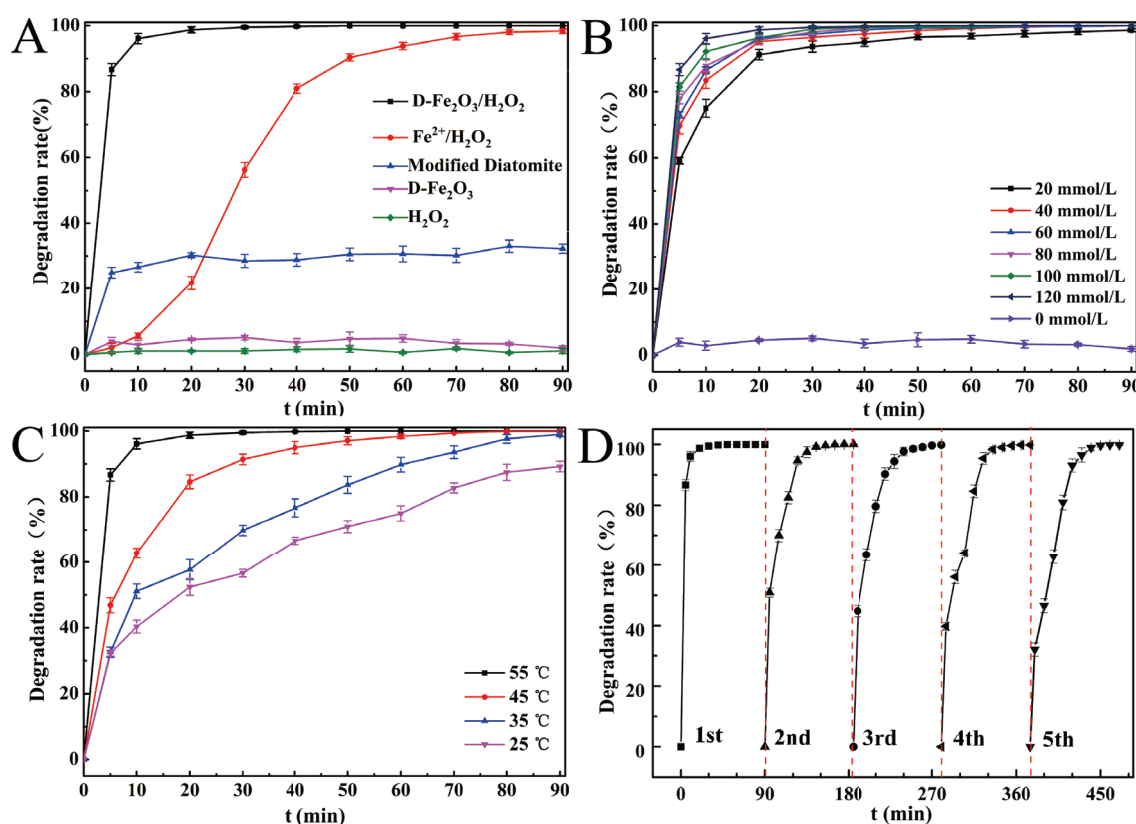


Fig. 5. A) The MB degradation efficiency in various systems; B) The effect of H<sub>2</sub>O<sub>2</sub> concentration on degradation of MB; C) The effect of temperature on the degradation of MB; D) The reusability of the D-Fe<sub>2</sub>O<sub>3</sub> catalyst.

dosage, the decoloration ratio enhanced with increasing  $H_2O_2$  dosage since it provided more radical sources [25,26]. However, the degradation rate grew slowly due to partial decomposition of  $H_2O_2$  in solution. Based on the experimental data and reported literature [24], possible reaction pathways has been proposed as follows.



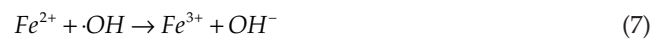
### 3.2.3. Effect of the reaction temperature

The reaction temperature effect was evaluated at  $D-Fe_2O_3$  dosage of 12 g/L, an initial pH of 3,  $H_2O_2$  concentration of 120 mmol/L, and a reaction temperature of 25, 35, 45, 55°C, respectively. As illustrated in Fig. 5C, the reaction temperature was crucial in heterogeneous Fenton system. High temperature, which played an important role in homogeneous systems [27,28], could also be beneficial in heterogeneous Fenton as the kinetic constants for both radical production and  $Fe^{2+}/Fe^{3+}$  regeneration exponentially increased as the reaction temperature increased. The decoloration ratio was improved from 84% to 99% in 90 min as temperature increased and the degradation rate reached the highest level at 55°C. Since the  $H_2O_2$  decomposition and MB degradation processes are endothermic, the rising tempera-

ture not only improved the activation energy of the reactants but also increased the possibility of the collision and contact between molecules.

### 3.2.4. Effect of the catalyst dosage

The catalyst dosage effect was evaluated at 55°C, with a  $H_2O_2$  concentration of 120 mmol/L, an initial pH of 3 and with  $D-Fe_2O_3$  dosages of 2, 4, 6, 8, 10, 12 g/L, respectively. As illustrated in Fig. 6A, the degradation process accelerates and the time to reach equilibrium shortened as the dosage increased. In heterogeneous Fenton system, when the catalyst contacted with  $H_2O_2$  solution, iron could be slowly dissolved into liquid phase to form a Fenton reactant, which converted into iron ions. This was because the addition of catalyst provides more catalytic sites and ferric ions (Fig. 5B), thus accelerating the transformation of  $H_2O_2$  to hydroxyl radicals ( $\cdot OH$ ). The degradation rate enhanced quickly until the dosage added up to 6 g/L since the extra free ferric ions capture the radicals in solution according to Eq. (7).



### 3.2.5. Effect of the initial pH

The initial pH effect was evaluated at 55°C, with a  $D-Fe_2O_3$  dosage of 12 g/L, a  $H_2O_2$  dosage of 120 mmol/L,

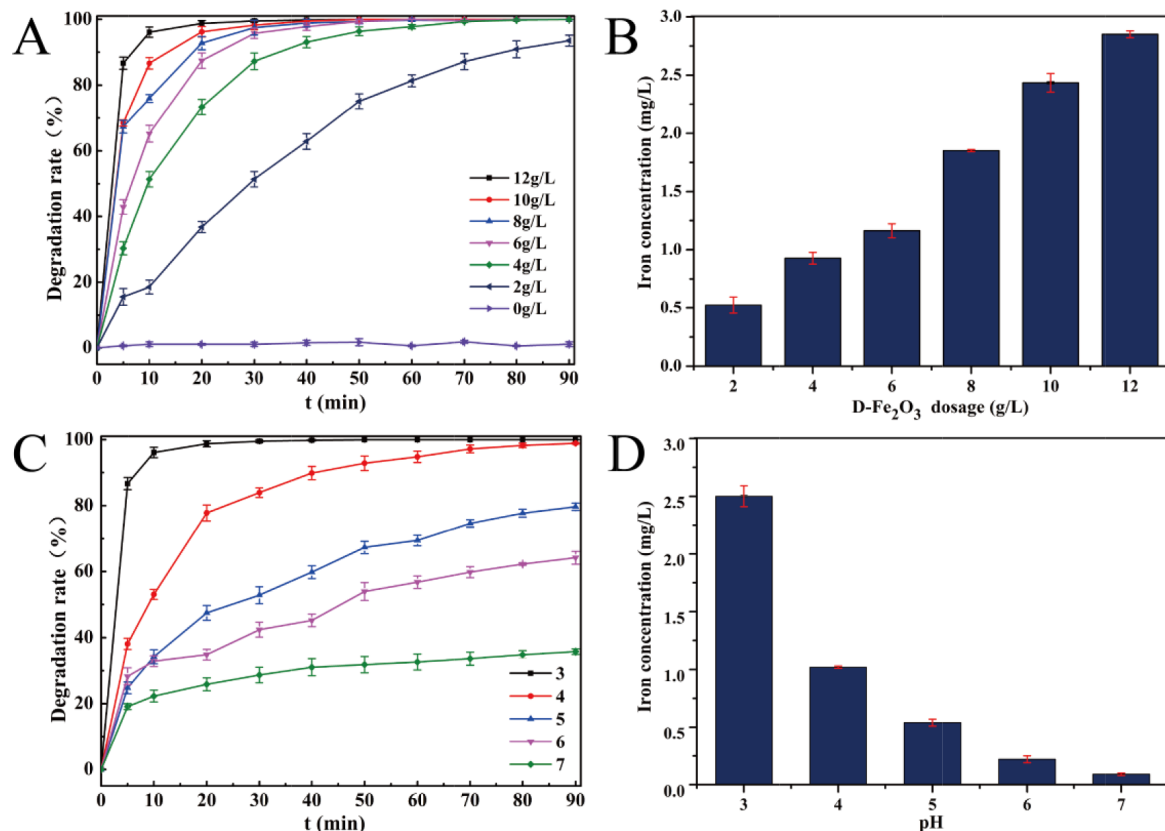


Fig. 6. A) The effect of  $D-Fe_2O_3$  dosage on the degradation of MB; B) The effect of  $D-Fe_2O_3$  dosage on the dissolved iron; C) The effect of pH on the degradation of MB; D) The effect of different pH on the dissolved iron.

and initial pH of 3, 4, 5, 6, and 7, respectively. According to Fig. 6C, 90% decoloration could be achieved in 20 min when the initial pH was 3 and the degradation rate drastically decreased by 33% as the initial pH increased to 7. This could be explained by the transformation of  $\text{Fe}_2\text{O}_3$  to  $\text{Fe}^{3+}$  that promoted oxidation of hydroxyl radicals in acidic conditions [29]. By increasing the pH value, the production of hydroxyl radicals and iron ions would be largely inhibited, the dissolved fraction of iron species decreased as colloidal ferric species appeared (Fig. 6D) [30]. The  $\text{H}_2\text{O}_2$  was unstable at high pH solution according to Eq. (8).



### 3.3. Reusability of diatomite- $\text{Fe}_2\text{O}_3$ catalyst

The reusability was evaluated at 55°C, with a D- $\text{Fe}_2\text{O}_3$  dosage of 12 g/L, a  $\text{H}_2\text{O}_2$  dosage of 120 mmol/L, and an initial pH of 3. The diatomite- $\text{Fe}_2\text{O}_3$  catalyst could be easily separated from the reaction solution by filtration. Prior to each reuse, the catalyst was washed with deionized water and ethanol for several times, and dried at 60°C immediately. As shown in Fig. 5D, the concentration of MB during the first run decreased by 99% during 30 min. After five cycles, the decoloration rate moderately slowed down in first 40 min. This was because the loaded  $\text{Fe}_2\text{O}_3$  reacted with  $\text{H}_2\text{O}_2$  and transforms to  $\text{Fe}^{3+}$ , and the amount of insoluble iron gradually decreased after every use. However, the complete degradation could still be reached within 50 min. The prepared D- $\text{Fe}_2\text{O}_3$  material did not show any significant loss of catalysis activity, indicating that the catalyst has a good stability and great application potential.

### 3.4. The kinetic analysis of MB degradation

To measure the decomposition of MB in the  $\text{H}_2\text{O}_2$ /D- $\text{Fe}_2\text{O}_3$  system, the samples were collected at given reaction times and analyzed immediately using a UV-vis spectrophotometer at 665 nm. According to Fig. 7, the intensity of the characteristic peak decreased gradually with the reaction time, indicating that the chromophores of MB were damaged.

For quantitative analysis, the kinetics of the decolorization of MB was simulated using a pseudo-first order kinetic model (Fig. 8). In the heterogeneous Fenton system, the reaction between  $\text{Fe}^{2+}/\text{Fe}^{3+}$  and  $\text{H}_2\text{O}_2$  occurred mainly at the solid catalyst surface. Therefore, the catalytic activity was largely determined by its specific surface area. By fitting data points using these equations, the initial rate constants ( $k$ ,  $\text{min}^{-1}$ ) of the reaction were calculated to be 0.033, 0.073, 0.117, 0.147, 0.172, and 0.246  $\text{min}^{-1}$ , respectively.

The reaction rate enhanced with the catalyst dosage. This was because the  $\text{H}_2\text{O}_2$  molecules could be captured by increasing the  $\text{Fe}_2\text{O}_3$  nanoparticles on surface of the catalyst and be transformed to hydroxyl radical ( $\cdot\text{OH}$ ). Subsequently, the free radicals oxidatively damage and further mineralize the MB molecules. As the key material in the catalysis, iron catalytically enhances the productivity of hydroxyl radicals leading to the increase of the reaction rate. Increasing diatomite- $\text{Fe}_2\text{O}_3$  dosage provides more catalytic sites and iron ions, thus accelerating the degradation process.

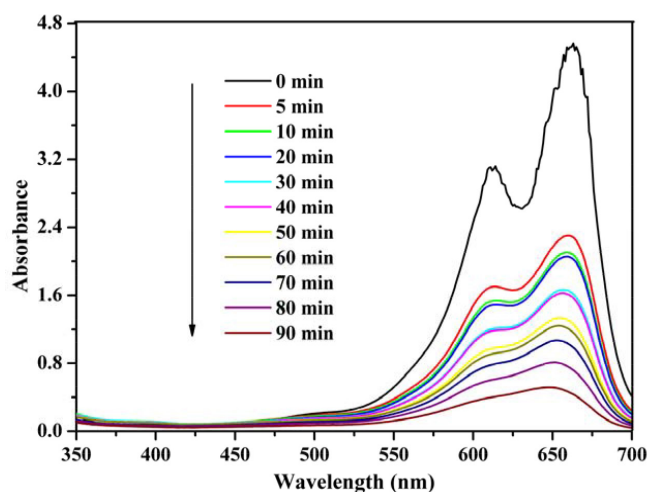


Fig. 7. UV-vis spectra of MB solutions at different time intervals during the typical degradation process using  $\text{H}_2\text{O}_2$ /D- $\text{Fe}_2\text{O}_3$  system.

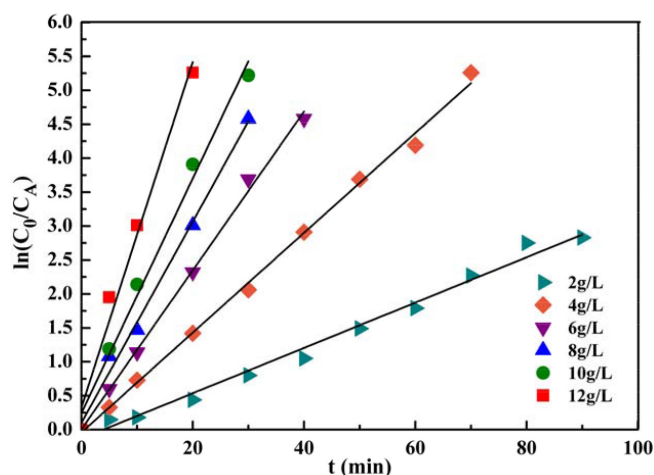


Fig. 8. The curve-fitting of MB degradation kinetics at different D- $\text{Fe}_2\text{O}_3$  dosage.

## 4. Conclusions

In this paper, the efficient heterogeneous Fenton catalyst diatomite- $\text{Fe}_2\text{O}_3$  has been successfully prepared by a simple impregnation strategy, as verified by SEM and EDX characterizations. The novel and highly efficient catalytic oxidation system of diatomite/ $\text{Fe}_2\text{O}_3$  is a promising catalyst for the rapid removal of cationic-dye in textile wastewater. The diatomite- $\text{Fe}_2\text{O}_3$  catalyst is highly effective for complete decoloration of MB (50 mg/L) in aqueous solution supplied with  $\text{H}_2\text{O}_2$ . This excellent catalytic performance is attributed to the highly porous morphology of diatomite, which acts as the host matrix for  $\text{Fe}_2\text{O}_3$ . Its porous morphology greatly increases the reaction area resulting in a highly efficient catalytic activity. The mechanism of cationic dye degradation is mainly attributed to the formation of hydroxyl radicals that are produced on the surface of the catalyst as a result of heterogeneous Fenton reactions. These findings provide new and practical approaches for textile wastewater treatment.

## Acknowledgments

This work was supported by the National Natural Science Foundation of China (51408074) and the Research Fund of State Key Laboratory of Geohazard Prevention and Geoenvironment Protection (No. SKLGP2015Z007). Dr. S.Y. Pu is grateful for support from the Hong Kong Scholars Program (No. XJ2015005) and the project funded by China Postdoctoral Science Foundation (2015T80966).

## Notes

The authors declare that there is no conflict of interests regarding the publication of this paper.

## References

- [1] A. Mittal, V. Thakur, J. Mittal, H. Vardhan, Process development for the removal of hazardous anionic azo dye Congo red from wastewater by using hen feather as potential adsorbent, *Desal. Water Treat.*, 52 (2014) 227–237.
- [2] S. Wang, A comparative study of Fenton and Fenton-like reaction kinetics in decolourisation of wastewater, *Dyes Pigments*, 76 (2008) 714–720.
- [3] S.M. Lam, J.C. Sin, A.R. Mohamed, A review on photocatalytic application of g-C<sub>3</sub>N<sub>4</sub>/semiconductor (CNS) nanocomposites towards the erasure of dyeing wastewater, *Mater. Sci. Semicond. Process.*, 47 (2016) 62–84.
- [4] S.S. Kumar, S. Shantkriti, T. Muruganandham, E. Murugesu, N. Rane, S.P. Govindwar, Bioinformatics aided microbial approach for bioremediation of wastewater containing textile dyes, *Ecol. Inform.*, 31 (2016) 112–121.
- [5] S. Popli, U.D. Patel, Destruction of azo dyes by anaerobic-aerobic sequential biological treatment: a review, *Int. J. Environ. Sci. Technol.*, 12 (2014) 405–420.
- [6] S.-y. Pu, L.-l. Qin, J.-p. Che, B.-r. Zhang, M. Xu, Preparation and application of a novel biofloculant by two strains of *Rhizopus* sp. using potato starch wastewater as nutrilit, *Bioresour. Technol.*, 162 (2014) 184–191.
- [7] J.J. Pignatello, E. Oliveros, A. MacKay, Advanced oxidation processes for organic contaminant destruction based on the Fenton reaction and related chemistry, *Crit. Rev. Environ. Sci. Technol.*, 36 (2006) 1–84.
- [8] A. Babuponnusami, K. Muthukumar, A review on Fenton and improvements to the Fenton process for wastewater treatment, *J. Environ. Chem. Eng.*, 2 (2014) 557–572.
- [9] Y. Yao, L. Wang, L. Sun, S. Zhu, Z. Huang, Y. Mao, W. Lu, W. Chen, Efficient removal of dyes using heterogeneous Fenton catalysts based on activated carbon fibers with enhanced activity, *Chem. Eng. Sci.*, 101 (2013) 424–431.
- [10] P.H. Ramos, F.A. La Porta, E.C. De Resende, J.O.S. Giacompo, M.C. Guerreiro, T.C. Ramalho, Fe-DPA as catalyst for oxidation of organic contaminants: evidence of homogeneous fenton process, *Z. für Anorganische Allgemeine Chemie*, 641 (2015) 780–785.
- [11] H. Zuniga-Benitez, G.A. Penuela, Degradation of ethylparaben under simulated sunlight using photo-Fenton, *Water Sci. Technol.*, 73 (2016) 818–826.
- [12] S. Navalon, M. Alvaro, H. Garcia, Heterogeneous Fenton catalysts based on clays, silicas and zeolites, *Appl. Catal. B: Environ.*, 99 (2010) 1–26.
- [13] H. Liang, S. Zhou, Y. Chen, F. Zhou, C. Yan, Diatomite coated with Fe<sub>2</sub>O<sub>3</sub> as an efficient heterogeneous catalyst for degradation of organic pollutant, *J. Taiwan Inst. Chem. Eng.*, 49 (2015) 105–112.
- [14] G. Sheng, G. Zhang, J. Wang, Photo-Fenton degradation of rhodamine B using Fe<sub>2</sub>O<sub>3</sub>-kaolin as heterogeneous catalyst: Characterization, process optimization and mechanism, *J. Colloid Interf. Sci.*, 433 (2014) 1–8.
- [15] H. Song, C. Chen, H. Zhang, J. Huang, Rapid decolorization of dyes in heterogeneous Fenton-like oxidation catalyzed by Fe-incorporated Ti-HMS molecular sieves, *J. Environ. Chem. Eng.*, 4 (2016) 460–467.
- [16] L. Zhou, J. Ma, Z. He, Y. Shao, Y. Li, Fabrication of magnetic carbon composites from peanut shells and its application as a heterogeneous Fenton catalyst in removal of methylene blue, *Appl. Surf. Sci.*, 324 (2015) 490–498.
- [17] H. Naeimi, Z.S. Nazifi, Sulfonated diatomite as heterogeneous acidic nanoporous catalyst for synthesis of 14-aryl-14-H-dibenzo a,j xanthenes under green conditions, *Appl. Catal. A-General*, 477 (2014) 132–140.
- [18] G. Zhang, B. Wang, Z. Sun, S. Zheng, S. Liu, A comparative study of different diatomite-supported TiO<sub>2</sub> composites and their photocatalytic performance for dye degradation, *Desal. Water Treat.*, 57 (2016) 17512–17522.
- [19] C.K.O. da Silva-Rackov, W.A. Lawal, P.A. Nfodzo, M.M.G.R. Vianna, C.A.O. do Nascimento, H. Choi, Degradation of PFOA by hydrogen peroxide and persulfate activated by iron-modified diatomite, *Appl. Catal. B-Environ.*, 192 (2016) 253–259.
- [20] N. Inchaurredo, C.P. Ramos, G. Zerjav, J. Font, A. Pintar, P. Haure, Modified diatomites for Fenton-like oxidation of phenol, *Micropor. Mesopor. Mater.*, 239 (2017) 396–408.
- [21] Y.M. Zha, Z.Q. Zhou, H.B. He, T.L. Wang, L.Q. Luo, Nanoscale zero-valent iron incorporated with nanomagnetic diatomite for catalytic degradation of methylene blue in heterogeneous Fenton system, *Water Sci. Technol.*, 73 (2016) 2815–2823.
- [22] W. Pranees, S. Neramittagapong, P. Assawasaengrat, A. Neramittagapong, Methanol dehydration to dimethyl ether over strong-acid-modified diatomite catalysts, *Energy Sources Part A-Recov. Utiliz. Environ. Effects*, 38 (2016) 3109–3115.
- [23] M. Bayat, M. Sohrabi, S.J. Royaei, Degradation of phenol by heterogeneous Fenton reaction using Fe/clinoptilolite, *J. Ind. Eng. Chem.*, 18 (2012) 957–962.
- [24] A.R. Khataee, S.G. Pakdehi, Removal of sodium azide from aqueous solution by Fenton-like process using natural laterite as a heterogeneous catalyst: Kinetic modeling based on nonlinear regression analysis, *J. Taiwan Inst. Chem. Eng.*, 45 (2014) 2664–2672.
- [25] M. Tekbaş, H.C. Yatmaz, N. Bektaş, Heterogeneous photo-Fenton oxidation of reactive azo dye solutions using iron exchanged zeolite as a catalyst, *Micropor. Mesopor. Mater.*, 115 (2008) 594–602.
- [26] J.H. Ramirez, M. Lampinen, M.A. Vicente, A. Carlos, A. Costa, L.M. Madeira, Experimental design to optimize the oxidation of orange II dye Solution using a clay-based Fenton-like catalyst, *Ind. Eng. Chem. Res.*, 47 (2007) 284–294.
- [27] Q. Liao, J. Sun, L. Gao, Degradation of phenol by heterogeneous Fenton reaction using multi-walled carbon nanotube supported Fe<sub>2</sub>O<sub>3</sub> catalysts, *Colloids Surf. A Physicochem. Eng. Asp.*, 345 (2009) 95–100.
- [28] A.A. Burbano, D.D. Dionysiou, M.T. Suidan, T.L. Richardson, Oxidation kinetics and effect of pH on the degradation of MTBE with Fenton reagent, *Water Res.*, 39 (2005) 107–118.
- [29] R.J. Watts, P.C. Stanton, J. Howsawkung, A.L. Teel, Mineralization of a sorbed polycyclic aromatic hydrocarbon in two soils using catalyzed hydrogen peroxide, *Water Res.*, 36 (2002) 4283–4292.